Journal of Sound and Vibration 329 (2010) 733–751

Contents lists available at ScienceDirect

Journal of Sound and Vibration

journal homepage: www.elsevier.com/locate/jsvi

Free vibrational characteristics of isotropic coupled cylindrical–conical shells

Mauro Caresta *, Nicole J. Kessissoglou

School of Mechanical and Manufacturing Engineering, The University of New South Wales, Sydney NSW 2052, Australia

ARTICLE INFO

Article history:
Received 11 March 2009
Received in revised form
29 September 2009
Accepted 4 October 2009
Handling Editor: L.G. Tham
Available online 28 October 2009

ABSTRACT

This paper presents the free vibrational characteristics of isotropic coupled conical–cylindrical shells. The equations of motion for the cylindrical and conical shells are solved using two different methods. A wave solution is used to describe the displacements of the cylindrical shell, while the displacements of the conical sections are solved using a power series solution. Both Donnell–Mushtari and Flügge equations of motion are used and the limitations associated with each thin shell theory are discussed. Natural frequencies are presented for different boundary conditions. The effect of the boundary conditions and the influence of the semi-vertex cone angle are described. The results from the theoretical model presented here are compared with those obtained by previous researchers and from a finite element model.

1. Introduction

Cylindrical shells are widely reported in literature. Many researchers such as Donnell–Mushtari, Timoshenko, Reissner, Flügge, to name a few, have developed thin shell theory arising from different simplifying assumptions based on Love's postulates. A range of general solutions for the cylindrical shell displacements and results for different boundary conditions have been summarised by Leissa [1]. Conical shells have not been as widely reported in literature as in the case of cylindrical shells. This is due to the increased mathematical complexity associated with the effect of the variation of the radius along the length of the cone on the elastic waves. The approximate location of the natural frequencies for conical shells has been found using the Rayleigh–Ritz method by several authors [1–5]. A transfer matrix approach was used by Irie et al. [6] to solve the free vibration of conical shells. Tong [7] presented a procedure for the free vibration analysis of isotropic and orthotropic conical shells in the form of a power series. Guo [8] studied the propagation and radiation properties of elastic waves in conical shells.

Very little work can be found on the vibrations of coupled cylindrical–conical shells, of which common applications are submarine hulls, aircraft, missiles and autonomous underwater vehicles (AUVs). Early analytical and experimental work to determine the natural frequencies and mode shapes of coupled conical–cylindrical shells used the finite element method [9]. The classic bending theory was used by Kalnins [10] and Rose et al. [11] to examine rotationally symmetric shells. Hu and Raney [12] examined the effects of discontinuities at the joint connecting the cone and cylinder. A transfer matrix approach was used by Irie et al. [13] to solve the free vibration of coupled cylindrical–conical shells. Efraim and Eisenberger [14] applied a power series solution to calculate the natural frequencies of segmented axisymmetric shells. Patel et al. [15] presented results for laminated composite joined conical–cylindrical shells using a finite element method.

* Corresponding author.
E-mail address: maurorestaca@yahoo.it (M. Caresta).

0022-460X/$ - see front matter © 2009 Elsevier Ltd. All rights reserved.
doi:10.1016/j.jsv.2009.10.003

In this work, the authors present a different approach to describe the free vibrational characteristics of coupled isotropic cylindrical–conical shells. The equations of motion for the cylindrical and conical shells are solved using two different methods. The cylindrical shell equations are solved using a wave solution while the conical shell equations are solved using a power series solution. These two methods are merged together for the first time to describe the dynamic response of the coupled shells. Two thin shell theories are used corresponding to Donnell–Mushtari and the higher order equations of Flügge. In the latter case it is shown that an approximation is required in order to apply the power series solution for the conical shell. Results in terms of natural frequencies and mode shapes are compared with data available in literature. The effect of the junction between the coupled shells and the boundary conditions is also investigated.

2. Equations of motion for thin shells

The equations of motion to describe the vibrations of cylindrical or conical shells can be derived according to a particular thin shell theory using the standard derivation [1]. For completeness of the present study, the derivation of thin shell theory is briefly reviewed in Appendix A.

2.1. Equations of motion for a cylindrical shell

Using a cylindrical coordinate system (x, θ), u, v and w are the orthogonal components of the shell displacement in the axial, circumferential and radial directions, respectively, as shown in Fig. 1. According to Flügge theory, the equations of motion for a thin cylindrical shell are

$$\frac{\partial^2 u}{\partial x^2}+\frac{(1-\upsilon)}{2a^2}(1+\beta^2)\frac{\partial^2 u}{\partial \theta^2}+\frac{(1+\upsilon)}{2a}\frac{\partial^2 v}{\partial x\,\partial \theta}+\frac{\upsilon}{a}\frac{\partial w}{\partial x}-\beta^2 a\frac{\partial^3 w}{\partial x^3}+\beta^2\frac{(1-\upsilon)}{2a}\frac{\partial^3 w}{\partial x\,\partial \theta^2}-\frac{1}{c_L^2}\frac{\partial^2 u}{\partial t^2}=0 \tag{1}$$

$$\frac{(1+\upsilon)}{2a}\frac{\partial^2 u}{\partial x\,\partial \theta}+\frac{(1-\upsilon)}{2}\frac{\partial^2 v}{\partial x^2}+\frac{1}{a^2}\frac{\partial^2 v}{\partial \theta^2}+\frac{1}{a^2}\frac{\partial w}{\partial \theta}+\beta^2\left(\frac{3(1-\upsilon)}{2}\frac{\partial^2 v}{\partial x^2}-\frac{(3-\upsilon)}{2}\frac{\partial^3 w}{\partial x^2\,\partial \theta}\right)-\frac{1}{c_L^2}\frac{\partial^2 v}{\partial t^2}=0 \tag{2}$$

$$\begin{aligned}&\beta^2\left(a^2\frac{\partial^4 w}{\partial x^4}+2\frac{\partial^4 w}{\partial x^2\,\partial \theta^2}+\frac{1}{a^2}\frac{\partial^4 w}{\partial \theta^4}-a\frac{\partial^3 u}{\partial x^3}+\frac{1-\upsilon}{2a}\frac{\partial^3 u}{\partial x\,\partial \theta^2}-\frac{(3-\upsilon)}{2}\frac{\partial^3 v}{\partial x^2\,\partial \theta}+\frac{2}{a^2}\frac{\partial^2 w}{\partial \theta^2}\right)\\&+\frac{\upsilon}{a}\frac{\partial u}{\partial x}+\frac{1}{a^2}\left(\frac{\partial v}{\partial \theta}+w(1+\beta^2)\right)+\frac{1}{c_L^2}\frac{\partial^2 w}{\partial t^2}=0\end{aligned} \tag{3}$$

where a is the radius of the middle surface of the shell, $\beta=h/\sqrt{12}a$ is the thickness parameter, h is the shell thickness and $\phi=\partial w/\partial x$ is the slope. $c_L=[E/\rho(1-\upsilon^2)]^{1/2}$ is the longitudinal wave speed. For Donnell–Mushtari theory, the equations of motion simplify to

$$\frac{\partial^2 u}{\partial x^2}+\frac{(1-\upsilon)}{2a^2}\frac{\partial^2 u}{\partial \theta^2}+\frac{(1+\upsilon)}{2a}\frac{\partial^2 v}{\partial x\,\partial \theta}+\frac{\upsilon}{a}\frac{\partial w}{\partial x}-\frac{1}{c_L^2}\frac{\partial^2 u}{\partial t^2}=0 \tag{4}$$

$$\frac{(1+\upsilon)}{2a}\frac{\partial^2 u}{\partial x\,\partial \theta}+\frac{(1-\upsilon)}{2}\frac{\partial^2 v}{\partial x^2}+\frac{1}{a^2}\frac{\partial^2 v}{\partial \theta^2}+\frac{1}{a^2}\frac{\partial w}{\partial \theta}-\frac{1}{c_L^2}\frac{\partial^2 v}{\partial t^2}=0 \tag{5}$$

$$\beta^2\left(a^2\frac{\partial^4 w}{\partial x^4}+2\frac{\partial^4 w}{\partial x^2\,\partial \theta^2}+\frac{1}{a^2}\frac{\partial^4 w}{\partial \theta^4}\right)+\frac{\upsilon}{a}\frac{\partial u}{\partial x}+\frac{1}{a^2}\frac{\partial v}{\partial \theta}+\frac{w}{a^2}+\frac{1}{c_L^2}\frac{\partial^2 w}{\partial t^2}=0 \tag{6}$$

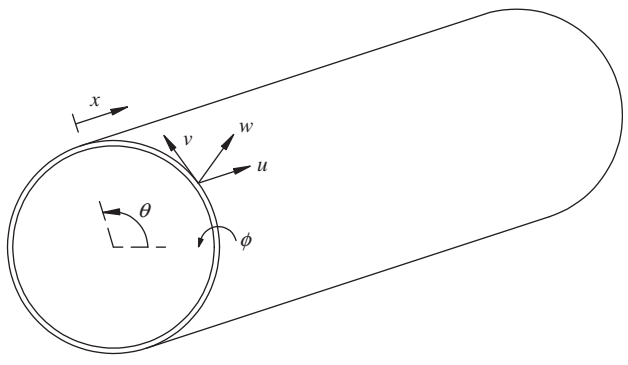

Fig. 1. Coordinate system for a thin walled cylindrical shell.

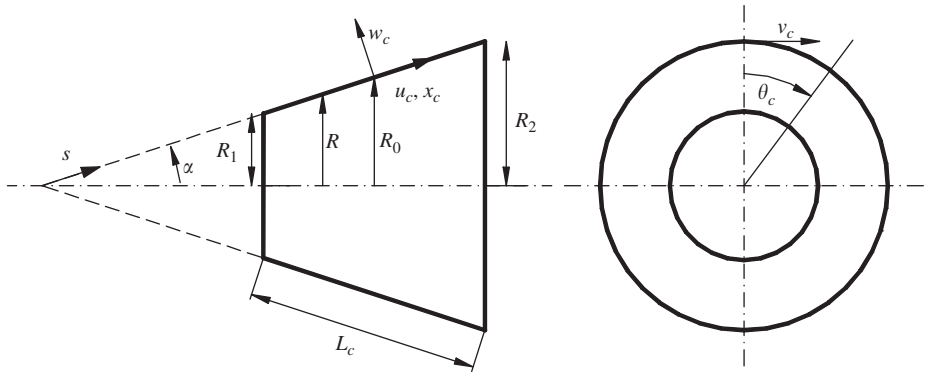

Fig. 2. Coordinate system for a thin walled conical shell.

2.2. Equations of motion for a conical shell

For a conical shell, the coordinate system (x_c, θ_c) is defined in Fig. 2. The equations of motion are given in terms of u_c and v_c that are the orthogonal components of the displacement in the x_c and θ_c directions, respectively. w_c is the displacement normal to the shell surface. α is the semi-vertex angle of the cone. s is the coordinate used in the standard derivation presented in Appendix A. R is the radius of the cone at location x_c. R_0 is the mean radius of the shell and corresponds to the origin of the coordinate system. L_c is the length of the cone along its generator, and R_1, R_2 are, respectively, the radii at the smaller and larger ends of the cone. According to Flügge theory, the equations of motion are

$$(L_{11}+\tilde{L}_{11})u_c + L_{12}v_c + (L_{13}+\tilde{L}_{13})w_c - \frac{1}{c_{cL}^2}\frac{\partial^2 u_c}{\partial t^2} = 0 \tag{7}$$

$$L_{21}u_c + (L_{22}+\tilde{L}_{22})v_c + (L_{23}+\tilde{L}_{23})w_c - \frac{1}{c_{cL}^2}\frac{\partial^2 v_c}{\partial t^2} = 0 \tag{8}$$

$$(L_{31}+\tilde{L}_{31})u_c + (L_{32}+\tilde{L}_{32})v_c + (L_{33}+\tilde{L}_{33})w_c - \frac{1}{c_{cL}^2}\frac{\partial^2 w_c}{\partial t^2} = 0 \tag{9}$$

$c_{cL} = [E_c/\rho_c(1-\upsilon_c^2)]^{1/2}$ is the longitudinal wave speed. E_c, ρ_c and υ_c are, respectively, Young's modulus, density and Poisson's ratio. Using Donnell–Mushtari theory, the differential operators $\tilde{L}_{ij}$ are zero. The Flügge equations of motion are more complicated due to the numerous higher order terms. The differential operators L_{ij} and $\tilde{L}_{ij}$ are given in Appendix B.

3. Solutions to the equations of motion

The equations of motion for the cylindrical and conical shells are solved using two different methods, and are then merged together to provide the complete response of the coupled conical–cylindrical structure. The cylindrical shell equations are solved using a wave solution whilst the conical shell equations are solved using a power series method. Furthermore, expressions for the conical shell displacements are obtained for both the Donnell–Mushtari and Flügge theories.

3.1. General solutions for the cylindrical shell

General solutions to the equations of motion for a cylindrical shell can be assumed as [1]

$$u(x,\theta,t) = U\mathrm{e}^{\mathrm{j}k_n x}\cos(n\theta)\mathrm{e}^{-\mathrm{j}\omega t} \tag{10}$$

$$v(x,\theta,t) = V\mathrm{e}^{\mathrm{j}k_n x}\sin(n\theta)\mathrm{e}^{-\mathrm{j}\omega t} \tag{11}$$

$$w(x,\theta,t) = W\mathrm{e}^{\mathrm{j}k_n x}\cos(n\theta)\mathrm{e}^{-\mathrm{j}\omega t} \tag{12}$$

where k_n is the axial wavenumber and n is the circumferential mode number. Substituting the general solutions given by Eqs. (10)–(12) into the Flügge equations of motion given by Eqs. (1)–(3) results in three linear equations in terms of U, V and W. These linear equations can be arranged in matrix form as $\mathbf{AU} = \mathbf{0}$, where $\mathbf{U} = [U\ V\ W]^{\mathrm{T}}$ contains the unknown wave amplitudes. The elements of the matrix $\mathbf{A}$ are given in Appendix C. For a non-trivial solution, the determinant of the matrix $\mathbf{A}$ must be zero. The expanded determinant results in an eighth order characteristic equation in k_n. For each value of

$k_{n,i}$ $(i=1:8)$, the axial and circumferential amplitude ratios can be obtained as $C_{n,i}=U_{n,i}/W_{n,i}$ and $G_{n,i}=V_{n,i}/W_{n,i}$, respectively. For harmonic motion, the complete solutions are given by

$$u(x,\theta,t)=\sum_{n=0}^{\infty}\sum_{i=1}^{8}C_{n,i}W_{n,i}e^{jk_{n,i}x}\cos(n\theta)e^{-j\omega t} \tag{13}$$

$$v(x,\theta,t)=\sum_{n=0}^{\infty}\sum_{i=1}^{8}G_{n,i}W_{n,i}e^{jk_{n,i}x}\sin(n\theta)e^{-j\omega t} \tag{14}$$

$$w(x,\theta,t)=\sum_{n=0}^{\infty}\sum_{i=1}^{8}W_{n,i}e^{jk_{n,i}x}\cos(n\theta)e^{-j\omega t} \tag{15}$$

3.2. General solutions for the conical shell

The equations of motion for the conical shell are solved using the power series approach presented by Tong [7] for shallow shell theory. This approach is applied here to the equations of motion for both the Donnell–Mushtari and the Flügge thin shell theories. General solutions to the equations of motion for a conical shell given by Eqs. (7)–(9) can be expressed as

$$u_c(x_c,\theta_c,t)=u_c(x_c)\cos(n\theta_c)e^{-j\omega t} \tag{16}$$

$$v_c(x_c,\theta_c,t)=v_c(x_c)\sin(n\theta_c)e^{-j\omega t} \tag{17}$$

$$w_c(x_c,\theta_c,t)=w_c(x_c)\cos(n\theta_c)e^{-j\omega t} \tag{18}$$

where the x_c-dependent component of the displacement can be expressed in terms of a power series by

$$u_c(x_c)=\sum_{m=0}^{\infty}a_m x_c^m \tag{19}$$

$$v_c(x_c)=\sum_{m=0}^{\infty}b_m x_c^m \tag{20}$$

$$w_c(x_c)=\sum_{m=0}^{\infty}c_m x_c^m \tag{21}$$

Solutions for the conical shell displacements for the two thin shell theories are presented in what follows.

3.2.1. Donnell–Mushtari equations

Using the low order Donnell–Mushtari theory, the equations of motion given by Eqs. (7) and (8) (and where the differential operators $\tilde{L}_{ij}$ are zero) are multiplied by R^2 while Eq. (9) is multiplied by R^4 [7], resulting in

$$R^2L_{11}u_c+R^2L_{12}v_c+R^2L_{13}w_c-\frac{R^2}{c_{cL}^2}\frac{\partial^2u_c}{\partial t^2}=0 \tag{22}$$

$$R^2L_{21}u_c+R^2L_{22}v_c+R^2L_{23}w_c-\frac{R^2}{c_{cL}^2}\frac{\partial^2v_c}{\partial t^2}=0 \tag{23}$$

$$R^4L_{31}u_c+R^4L_{32}v_c+R^4L_{33}w_c-\frac{R^4}{c_{cL}^2}\frac{\partial^2w_c}{\partial t^2}=0 \tag{24}$$

Substituting Eqs. (16)–(21) into Eqs. (22)–(24) results in the following recurrence relations for $m=0,1,2,\ldots$:

$$a_{m+2}=\sum_{i=1}^{4}A_{a,i}a_{m-3+i}+\sum_{i=1}^{2}B_{a,i}b_{m-1+i}+\sum_{i=1}^{2}C_{a,i}c_{m-1+i} \tag{25}$$

$$b_{m+2}=\sum_{i=1}^{2}A_{b,i}a_{m-1+i}+\sum_{i=1}^{4}B_{b,i}b_{m-3+i}+C_{b,1}c_m \tag{26}$$

$$c_{m+4}=\sum_{i=1}^{4}A_{c,i}a_{m-3+i}+\sum_{i=1}^{3}B_{c,i}b_{m-3+i}+\sum_{i=1}^{8}C_{c,i}c_{m-5+i} \tag{27}$$

The coefficients in Eqs. (25)–(27) are given in Appendix D.

3.2.2. Flügge equations

Using the Flügge equations, the application of the power series solution is more complicated compared with the Donnell–Mushtari theory due to the higher order terms. The coefficients of the operators L_{ij} and $\tilde{L}_{ij}$ $\{i,j=1:3\}$ include terms of the form $1/R^k$, k=1:4. Hence, the equations of motion given by Eqs. (17)–(19) are multiplied by R^4 in order to apply the power series solution. Furthermore, the terms with h^2 in the membrane force N_s given by Eq. (A.6), given in Appendix A, are neglected, as in the Donnell–Mushtari theory. The approximation of N_s results in a new $\tilde{L}_{13}$ term, given by

$$\tilde{L}_{13} = -\frac{h_c^2}{12}\frac{\sin^2\alpha\cos^3\alpha}{R^4} - \frac{h_c^2\sin^2\alpha\cos\alpha}{12R^3} + \frac{\partial}{\partial x_c}\frac{1-\upsilon_c}{2R}\frac{h_c^2}{12}\frac{\partial^3}{\partial x_c\,\partial\theta_c^2} - \frac{3-\upsilon}{2}\frac{h_c^2}{12}\frac{\sin\alpha\cos\alpha}{R^4}\frac{\partial^2}{\partial\theta_c^2} \tag{28}$$

Substituting Eqs. (16)–(21) into Eqs. (7)–(9) (multiplied by R^4) results in the following recurrence relations for $m=0,1,2,\ldots$:

$$a_{m+2} = \sum_{i=1}^{6}\tilde{A}_{a,i}a_{m-5+i} + \sum_{i=1}^{4}\tilde{B}_{a,i}b_{m-3+i} + \sum_{i=1}^{4}\tilde{C}_{a,i}c_{m-3+i} \tag{29}$$

$$b_{m+2} = \sum_{i=1}^{4}\tilde{A}_{b,i}a_{m-3+i} + \sum_{i=1}^{6}\tilde{B}_{b,i}b_{m-5+i} + \sum_{i=1}^{5}\tilde{C}_{b,i}c_{m-3+i} \tag{30}$$

$$c_{m+4} = \sum_{i=1}^{6}\tilde{A}_{c,i}a_{m-3+i} + \sum_{i=1}^{5}\tilde{B}_{c,i}b_{m-3+i} + \sum_{i=1}^{8}\tilde{C}_{c,i}c_{m-5+i} \tag{31}$$

The recurrence coefficients in Eqs. (29)–(31) are given in Appendix E. It is important to note that if the h^2 term in Eq. (A.6) is not neglected, the power series method cannot be applied since the recurrence relation given by Eq. (29) would become

$$a_{m+2} = \sum_{i=1}^{6}\tilde{A}_{a,i}a_{m-5+i} + \sum_{i=1}^{4}\tilde{B}_{a,i}b_{m-3+i} + \sum_{i=1}^{6}\tilde{C}_{a,i}c_{m-3+i} \tag{32}$$

The new terms c_{m+2} and c_{m+3} are not compatible with the term a_{m+2} on the left side of the equation. It can be concluded that the use of the power series solution with the Flügge equations is only possible if the approximated membrane force N_s, as in the Donnell–Mushtari theory, is used.

3.2.3. Conical shell displacements

Tong [7] showed that the x_c-dependent part of the displacements can be expressed in terms of eight unknown coefficients $a_0, a_1, b_0, b_1, c_0, c_1, c_2, c_3$, which can be determined from the boundary conditions at both ends on the conical shell. In terms of the unknown coefficients, Eqs. (19)–(21) can be written as follows:

$$u_c(x_c) = \mathbf{u}\cdot\mathbf{x}, \quad v_c(x_c) = \mathbf{v}\cdot\mathbf{x}, \quad w_c(x_c) = \mathbf{w}\cdot\mathbf{x} \tag{33}$$

where

$$\mathbf{u} = [u_1(x_c) \;\; \cdots \;\; u_8(x_c)] \tag{34}$$

$$\mathbf{v} = [v_1(x_c) \;\; \cdots \;\; v_8(x_c)] \tag{35}$$

$$\mathbf{w} = [w_1(x_c) \;\; \cdots \;\; w_8(x_c)] \tag{36}$$

$$\mathbf{x} = [a_0 \;\; a_1 \;\; b_0 \;\; b_1 \;\; c_0 \;\; c_1 \;\; c_2 \;\; c_3]^{\mathrm{T}} \tag{37}$$

$\mathbf{x}$ is the vector of the eight unknown coefficients. In Eqs. (34)–(36), $u_i(x_c)$, $v_i(x_c)$ and $w_i(x_c)$ are the base functions of $u_c(x_c)$, $v_c(x_c)$ and $w_c(x_c)$, respectively. The convergence property of the series solutions $u_c(x_c)$, $v_c(x_c)$, $w_c(x_c)$ given by Eqs. (19)–(21) has been previously discussed by Tong [7] and are maintained for the thin-shell theories presented here.

4. Boundary and continuity conditions

The two different methods corresponding to the wave solution and power series method both require the application of four boundary conditions at each end of the shell to determine the unknown coefficients. Thus, the cylindrical and conical shells can be coupled together by applying the required continuity and equilibrium conditions at the interface. The remaining boundary conditions are applied at the ends of the coupled cylindrical–conical shell. The forces, moments and displacements at the junction and at the boundaries of the coupled shells are given in accordance with the sign

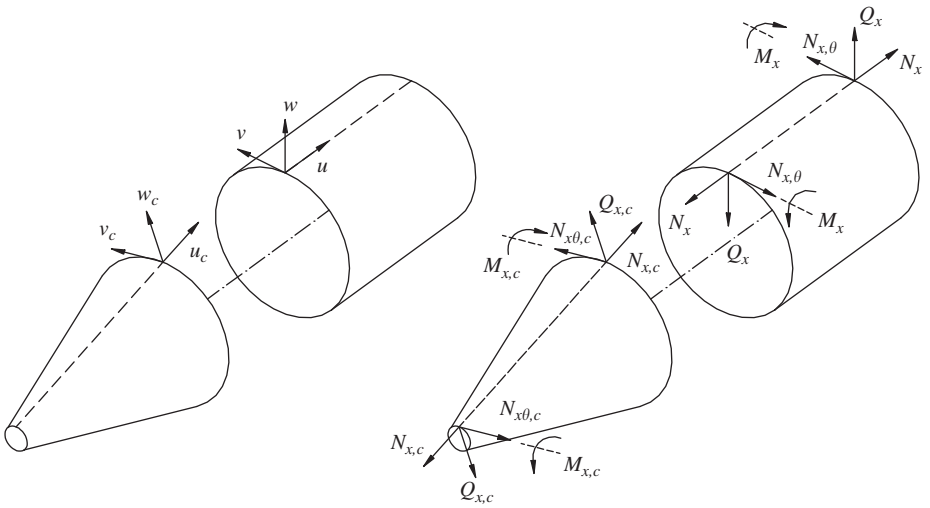

Fig. 3. Positive directions for the forces, moments and displacements of the cone and cylinder.

convention shown in Fig. 3. At the cylinder–cone junction, continuity of displacements, slope, forces and bending moment are given by

$$u = U_c \tag{38}$$

$$w = W_c \tag{39}$$

$$v = V_c \tag{40}$$

$$\frac{\partial w}{\partial x} = \frac{\partial w_c}{\partial x_c} \tag{41}$$

$$\tilde{N}_{x,c} - N_x = 0 \tag{42}$$

$$\left(N_{x\theta,c} + \frac{M_{x\theta,c}}{R_2}\right) - \left(N_{x\theta} + \frac{M_{x\theta}}{a}\right) = 0 \tag{43}$$

$$M_{x,c} - M_x = 0 \tag{44}$$

$$\tilde{V}_{x,c} - V_x = 0 \tag{45}$$

To take into account the change of curvature between the cylinder and the cone, the following notation was introduced:

$$U_c = u_c \cos\alpha - w_c \sin\alpha \tag{46}$$

$$W_c = u_c \sin\alpha + w_c \cos\alpha \tag{47}$$

$$\tilde{N}_{x,c} = N_{x,c} \cos\alpha - V_{x,c} \sin\alpha \tag{48}$$

$$\tilde{V}_{x,c} = V_{x,c} \cos\alpha + N_{x,c} \sin\alpha \tag{49}$$

The membrane forces N_x, N_θ and $N_{x\theta}$, bending moments M_x, M_θ and $M_{x\theta}$, transverse shearing Q_x and the Kelvin–Kirchhoff shear force V_x can be derived for both shells. Different boundary conditions can be applied to the extremities of the coupled shells. In this work, three different boundary conditions have been considered, corresponding to free, clamped and shear diaphragm. The various boundary conditions, for example for the cylindrical shell, are

$$\text{Free end} : N_x = \left(N_{x\theta} + \frac{M_{x\theta}}{a}\right) = M_x = V_x = 0 \tag{50}$$

$$\text{Clamped end} : u = w = \frac{\partial w}{\partial x} = v = 0 \tag{51}$$

$$\text{Shear-diaphragm (SD) end} : N_x = v = M_x = w = 0 \tag{52}$$

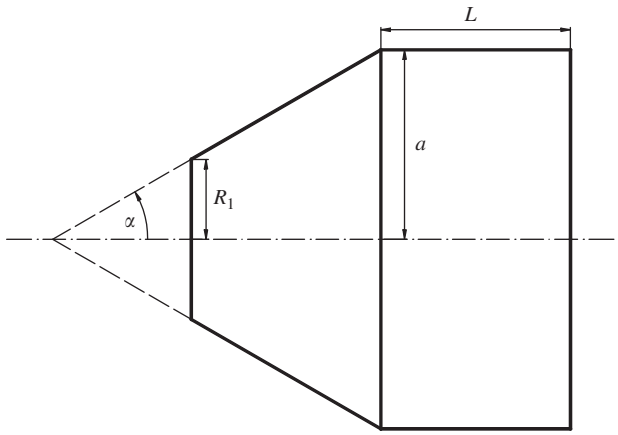

Fig. 4. Coupled cylindrical–conical shell.

Table 1
Frequency parameters for the free–clamped cylindrical–conical shell.

Mode order		Frequency parameter Ω_c			
n	η	Irie et al. [13]	Efraim et al. [14]	Present (Donnell–Mushtari)	Present (Flügge)
0	1	0.5047	0.503779	0.503752	0.505354
	T	–	0.609852	0.609855	0.609816
	2	0.9312	0.930942	0.930916	0.930904
	3	0.9566	0.956379	0.956315	0.956292
	4	0.9718	0.971634	0.971596	0.971538
	5	1.0122	1.012090	1.011884	1.011873
1	1	0.2930	0.292875	0.292908	0.293357
	2	0.6368	0.635834	0.635819	0.636844
	3	0.8116	0.811454	0.811446	0.811434
	4	0.9316	0.931565	0.931481	0.931458
	5	0.9528	0.952178	0.952189	0.952120
	6	0.9922	0.992175	0.991959	0.991936
2	1	0.1010	0.099968	0.102034	0.100087
	2	0.5032	0.502701	0.502899	0.502819
	3	0.6916	0.691305	0.691479	0.691353
	4	0.8592	0.859114	0.859017	0.858971
	5	0.9164	0.915870	0.916072	0.915877
	6	0.9608	0.960702	0.960475	0.960429
3	1	0.09076	0.087603	0.093771	0.087330
	2	0.3921	0.391569	0.392199	0.391450
	3	0.5148	0.514478	0.515184	0.514424
	4	0.7537	0.753402	0.753595	0.753295
	5	0.7970	0.796590	0.796983	0.796557
	6	0.9197	0.919635	0.919391	0.919369
4	1	0.1477	0.144619	0.150574	0.144478
	2	0.3312	0.330354	0.331698	0.330177
	3	0.3965	0.395649	0.397604	0.395495
	4	0.6473	0.646678	0.647700	0.646548
	5	0.6932	0.692805	0.693197	0.692690
	6	0.8720	0.871812	0.871555	0.871532
5	1	0.2021	0.199546	0.203896	0.199540
	2	0.2966	0.296020	0.296330	0.295939
	3	0.3730	0.370901	0.376227	0.370707
	4	0.5805	0.579750	0.581667	0.579581
	5	0.6138	0.613363	0.614222	0.613231
	6	0.8187	0.817951	0.819801	0.818014

'T' denotes the purely torsional frequency.

The four boundary conditions at each end of the coupled cylindrical–conical shell together with the eight continuity equations at the junction can be arranged in matrix form $\mathbf{BX} = \mathbf{0}$, where $\mathbf{X}$ is the vector of the 16 unknown coefficients given by

$$\mathbf{X} = [a_0 \;\; a_1 \;\; b_0 \;\; b_1 \;\; c_0 \;\; c_1 \;\; c_2 \;\; c_3 \;\; W_{n,1} \;\; \cdots \;\; W_{n,8}]^{\mathrm{T}} \tag{53}$$

The vanishing of the determinant of matrix $\mathbf{B}$ gives the undamped natural frequencies of the joined shells.

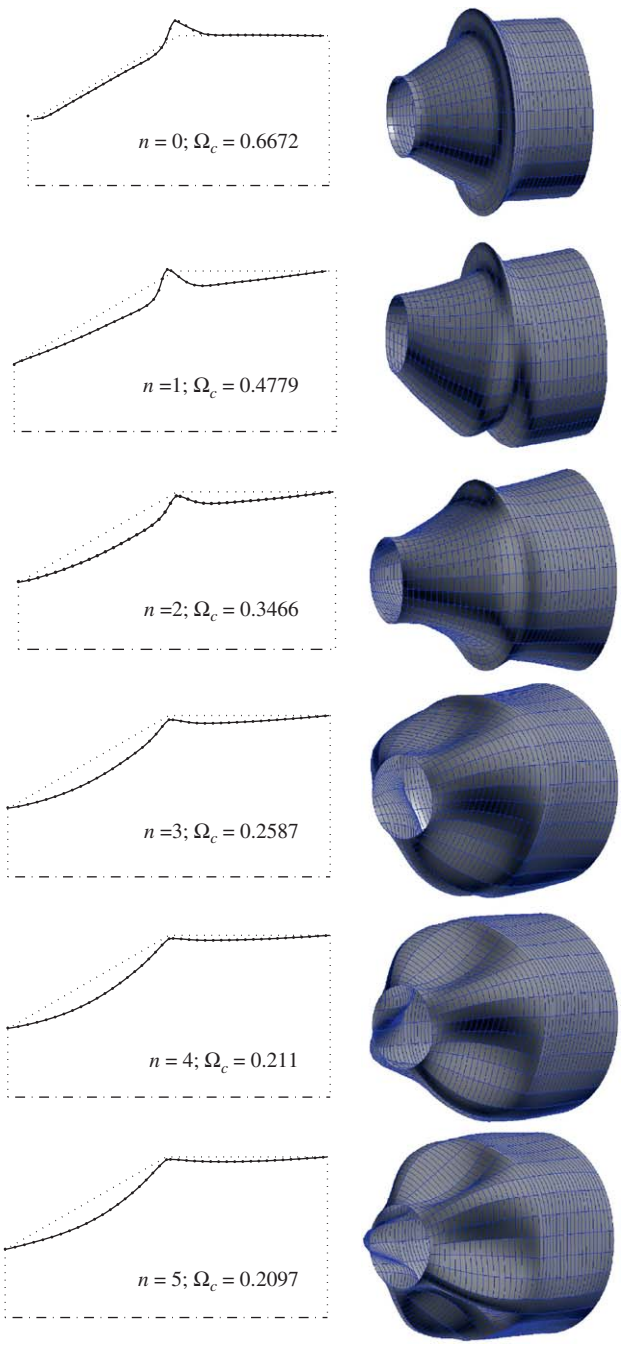

Fig. 5. Lowest order mode shapes corresponding to n=0:5 SD–SD case.

5. Results

5.1. Natural frequencies

To confirm the validity of the presented method, results available in Refs. [13,14] are reproduced here. A coupled cylindrical–conical shell shown in Fig. 4 with free boundary conditions at the cone end and a clamped boundary for the

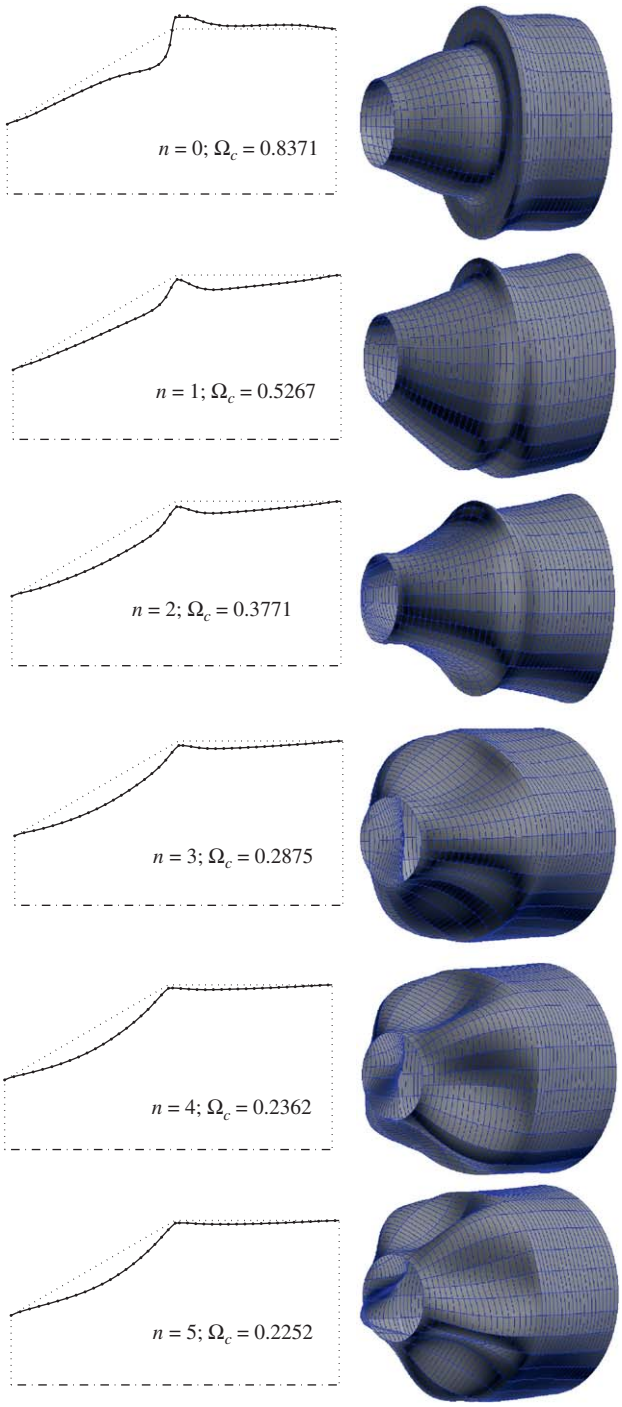

Fig. 6. Lowest order mode shapes corresponding to n=0:5 clamped–clamped case.

cylinder is examined, with the following data: $L/a = 1$, $h/a = 0.01$, $R_1/a = 0.4226$, $\alpha = 30^\circ$. The shells are of the same material with Young's modulus $E = 2.11 \times 10^{11}\,\mathrm{N\,m^{-2}}$, Poisson's ratio $\upsilon = 0.3$ and density $\rho = 7800\,\mathrm{kg\,m^{-3}}$.

The dimensionless frequency parameter $\Omega_c = \omega a/c_L$ for the lowest six values of the circumferential mode number ($n = 0, \ldots, 5$) are given in Table 1. The values of the frequency parameters agree well with those presented previously by Irie et al. [13] and Efraim et al. [14]. A very small difference is observed between the two shell theories except at lower frequencies, where the Donnell–Mushtari theory is not as accurate as the Flügge theory [1]. When n=0, the equation of motion for the circumferential displacement is uncoupled from the equations of motion for the axial and radial displacements for both the conical and cylindrical shells, yielding a purely torsional mode [1]. The frequency value of the mode with order $[n\ \ \eta] = [0\ \ T]$ corresponds to the first purely torsional mode. This frequency is omitted in the work of Irie et al. [13] since they did not consider the torsional solution. The purely torsional frequency is reported in Efraim et al.

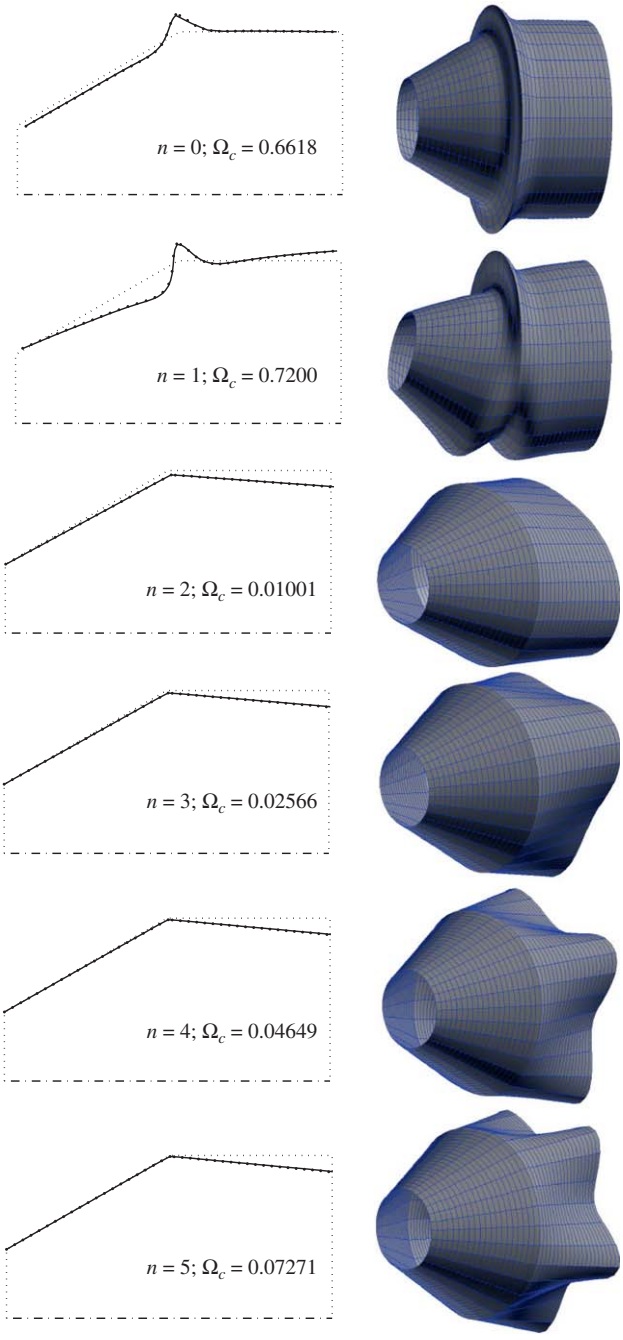

Fig. 7. Lowest order mode shapes corresponding to n=0:5 free–free case.

[14], but their corresponding mode shape appears to be in contrast with a purely torsional solution. To further validate the analytical method presented in this work, a computational finite element model (FEM) was developed using Patran/Nastran. Quadratic eight node (CQUAD8) elements were used for the 2D thin shell elements; the cylinder and the cone were meshed with 20 elements in the axial direction and 30 in the circumferential direction. The Lanczos extraction method was adopted in the analysis [16]. The lowest order mode shapes corresponding to n=0:5 for SD–SD, clamped–clamped and free–free boundary conditions have been normalised and are, respectively, shown in Figs. 5–7. The analytical results represented by the continuous line are practically indistinguishable to those obtained from the FE model (represented by dots). Screenshots of the mode shapes from the FE model are also shown. The mode shapes for the SD–SD and clamped–clamped cases are similar with a large deformation at the cylinder/cone junction for n=0. As the circumferential mode number increases, a larger deformation of the cone with respect to the cylinder can be observed. For the free–free case and n=0:1, the mode shapes show similar characteristics to the other boundary conditions while for $n \geq 2$, a larger deformation for the cylindrical shell is observed compared to the displacement of the conical section.

5.2. Effect of the boundary conditions

The effect of boundary conditions on the free vibrational characteristics of a coupled conical–cylindrical shell is examined. In Fig. 8, the lowest frequency parameter is plotted versus the circumferential mode number n. The frequencies calculated using both the Donnell–Mushtari and Flügge equations are compared with the results given by the FE model. A logarithmic scale was used to emphasize the small differences in the results. It can be seen that the results given by the Flügge equations of motion match almost perfectly with the FE results. The results given by the Donnell–Mushtari equations are affected by several issues for coupled cylindrical–conical shells. Firstly, it can be observed that they perform less well at low frequencies compared with the results given by both the Flügge equations of motion and the finite element model. Furthermore, they are in error for the free–free case. For this boundary condition, the equations for n=1 give two incorrect frequencies of very low values that should be the zeroes associated with rigid body rotation. This is due to the inconsistency of Donnell–Mushtari theory with free body motion, as reported by Kadi [17] and Kraus [18].

For clamped–clamped and SD–SD boundary conditions, the lowest frequency parameter decreases with n. For free–clamped boundary conditions, the frequencies initially decrease and then increase after n=3. For the free–free case, a very low frequency occurs at n=2.

5.3. Effect of the semi-vertex cone angle

Figs. 9–11 present the effect of the semi-vertex angle α of the conical shell on the frequency parameter Ω_c, for different boundary conditions of the coupled shell. The following data for the coupled shells were used: $L/a = 1$, $h/a = 0.01$, $L_c = 1$, $\alpha \in [0, 90^\circ]$. For extreme values of the semi-vertex angle corresponding to α=0° and 90°, the conical shell degenerates to a cylindrical shell and a circular plate, respectively. For the n=0 mode, the behaviour of the coupled shell is similar for all

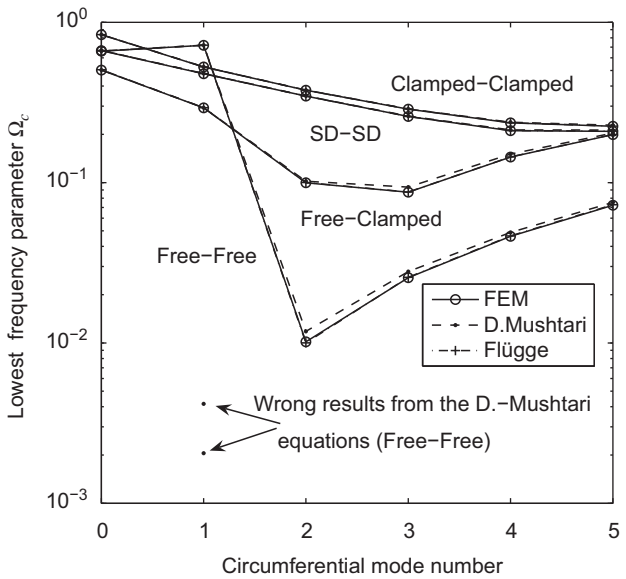

Fig. 8. Lowest frequency parameter Ω_c for different boundary conditions calculated using the Donnell–Mushtari and Flügge equations and compared with the results from an FE model.

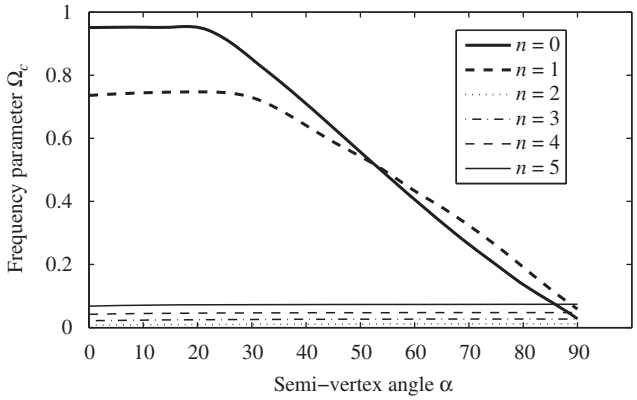

Fig. 9. Lowest frequency parameter Ω_c for free–free boundary conditions.

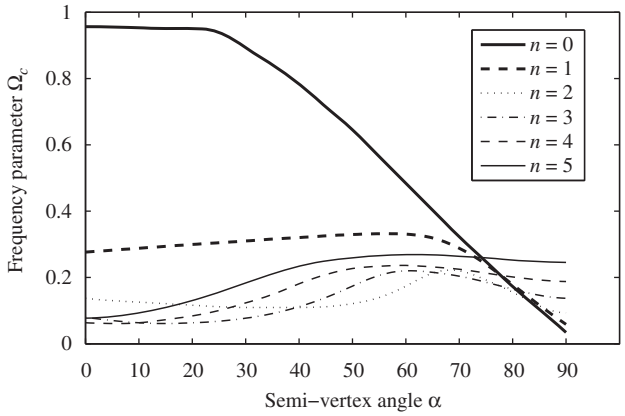

Fig. 10. Lowest frequency parameter Ω_c for free–clamped boundary conditions.

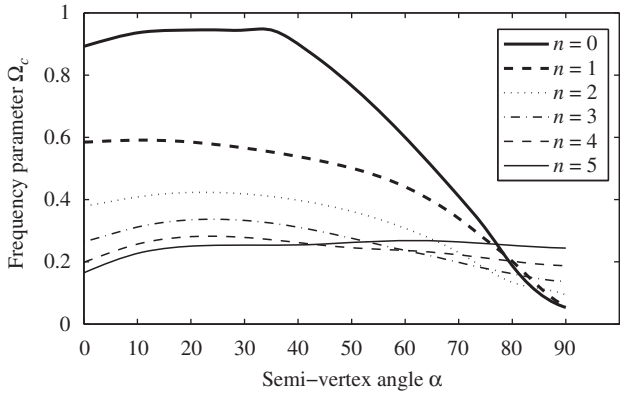

Fig. 11. Lowest frequency parameter Ω_c for clamped–clamped boundary conditions.

boundary conditions considered, resulting in a relatively constant value in the frequency parameter for increasing values of α and then a mainly linear decrease in Ω_c. The corresponding motion is primarily axial. As the conical shell changes from a cylindrical shell (at α=0) to a plate-like structure (at α=90°), a decrease in axial stiffness occurs resulting in a decrease in the frequency parameter. A similar behaviour to the n=0 mode is observed for the n=1 bending mode for a free–free coupled shell. For $n \geq 2$, the frequency parameter is almost constant for all values of α for the free–free shell. For a coupled shell with a free boundary at the conical shell end and clamped at the cylindrical shell end, for n=1 a slight increase of the frequency parameter with α is observed, showing a small mass effect. A stiffening effect then dominates after α=65°. In the free–clamped shell, higher order circumferential modes result in a wavelike behaviour due to greater shape complexity.

6. Conclusions

A different approach to obtain the free vibrational characteristics of coupled cylindrical–coupled shells has been introduced. Two different methods corresponding to a wave solution and power series method were used to obtain the shell displacements. The shells were then coupled by means of continuity conditions at the cone/cylinder junction. Results in terms of natural frequencies were compared for two different thin shell theories, corresponding to Donnell–Mushtari and Flügge equations, as well as with data presented previously in Refs. [13,14]. It was shown that in order to use the Flügge equations of motion with the power series solution, an approximation of the shear force is required. The effect of four classical boundary conditions at the ends of the coupled shells on the natural frequencies was investigated.

In general, little difference was observed between the results given by the two shell theories. The Flügge equations were shown to be in very close agreement with results from a finite element model, but the Donnell–Mushtari equations were less accurate at low frequencies. Furthermore, for free–free boundary conditions of the coupled shells, the Donnell–Mushtari equations generate errors in the values of the lowest frequency parameter for circumferential mode number n=1.

The method described in this work can also be applied to the coupled shells of different materials and thickness.

Appendix A. Equations of motion for thin isotropic shells

According to Flügge theory, the equations of motion for a thin shell are given by

$$\frac{\partial(BN_s)}{\partial s}+\frac{\partial(AN_{\theta s})}{\partial \theta}+\frac{\partial A}{\partial \theta}N_{s\theta}-\frac{\partial B}{\partial s}N_\theta+\frac{AB}{R_s}Q_s-AB\rho h\frac{\partial^2 u}{\partial t^2}=0 \tag{A.1}$$

$$\frac{\partial(AN_\theta)}{\partial \theta}+\frac{\partial(BN_{s\theta})}{\partial s}+\frac{\partial B}{\partial s}N_{\theta s}-\frac{\partial A}{\partial \theta}N_s+\frac{AB}{R_\theta}Q_\theta-AB\rho h\frac{\partial^2 v}{\partial t^2}=0 \tag{A.2}$$

$$-\frac{AB}{R_s}N_s-\frac{AB}{R_\theta}N_\theta+\frac{\partial(BQ_s)}{\partial s}+\frac{\partial(AQ_\theta)}{\partial \theta}-AB\rho h\frac{\partial^2 w}{\partial t^2}=0 \tag{A.3}$$

where u, v and w, respectively, denote the orthogonal component of the displacement. ρ is the density and h is the shell thickness. The equations are given in terms of two independent coordinates s and θ. The parameters A, B, R_s and R_θ depend on the type of shell. The forces and moments in Eqs. (A.1)–(A.3) are given by [1]

$$Q_s=\frac{1}{AB}\frac{\partial(BM_s)}{\partial s}+\frac{\partial(AM_{\theta s})}{\partial \theta}+\frac{\partial A}{\partial \theta}M_{s\theta}-\frac{\partial B}{\partial s}M_\theta \tag{A.4}$$

$$Q_\theta=\frac{1}{AB}\frac{\partial(AM_\theta)}{\partial \theta}+\frac{\partial(BM_{s\theta})}{\partial s}+\frac{\partial B}{\partial s}M_{\theta s}-\frac{\partial A}{\partial \theta}M_s \tag{A.5}$$

$$N_s=\frac{Eh}{1-\upsilon^2}\left[\varepsilon_s+\upsilon\varepsilon_\theta-\frac{h^2}{12}\left(\frac{1}{R_s}-\frac{1}{R_\theta}\right)\left(k_s-\frac{\varepsilon_s}{R_s}\right)\right] \tag{A.6}$$

$$N_\theta=\frac{Eh}{1-\upsilon^2}\left[\varepsilon_\theta+\upsilon\varepsilon_s-\frac{h^2}{12}\left(\frac{1}{R_\theta}-\frac{1}{R_s}\right)\left(k_\theta-\frac{\varepsilon_\theta}{R_\theta}\right)\right] \tag{A.7}$$

$$N_{s\theta}=\frac{Eh}{2(1+\upsilon)}\left[\varepsilon_{s\theta}-\frac{h^2}{12}\left(\frac{1}{R_s}-\frac{1}{R_\theta}\right)\left(\frac{\tau}{2}-\frac{\varepsilon_{s\theta}}{R_s}\right)\right] \tag{A.8}$$

$$N_{\theta s}=\frac{Eh}{2(1+\upsilon)}\left[\varepsilon_{s\theta}-\frac{h^2}{12}\left(\frac{1}{R_\theta}-\frac{1}{R_s}\right)\left(\frac{\tau}{2}-\frac{\varepsilon_{s\theta}}{R_\theta}\right)\right] \tag{A.9}$$

$$M_s=\frac{Eh^3}{12(1-\upsilon^2)}\left[k_s+\upsilon k_\theta-\left(\frac{1}{R_s}-\frac{1}{R_\theta}\right)\varepsilon_s\right] \tag{A.10}$$

$$M_\theta=\frac{Eh^3}{12(1-\upsilon^2)}\left[k_\theta+\upsilon k_s-\left(\frac{1}{R_\theta}-\frac{1}{R_s}\right)\varepsilon_\theta\right] \tag{A.11}$$

$$M_{s\theta}=\frac{Eh^3}{24(1+\upsilon)}\left(\tau-\frac{\varepsilon_{s\theta}}{R_s}\right) \tag{A.12}$$

$$M_{\theta s}=\frac{Eh^3}{24(1+\upsilon)}\left(\tau-\frac{\varepsilon_{s\theta}}{R_\theta}\right) \tag{A.13}$$

$$V_s=Q_s+\frac{1}{B}\frac{\partial M_{x\theta}}{\partial \theta} \tag{A.14}$$

E is Young's modulus and υ is Poisson's ratio of the material. Eq. (A.14) is the Kelvin–Kirchhoff shearing force. The normal strain ε_s, ε_θ, and shear strain $\varepsilon_{s\theta}$ of the middle surface and the rotations of the normal to the middle surface denoted by ϑ_s and ϑ_θ are given by

$$\varepsilon_s = \frac{1}{A}\frac{\partial u}{\partial s} + \frac{v}{AB}\frac{\partial A}{\partial \theta} + \frac{w}{R_s} \tag{A.15}$$

$$\varepsilon_\theta = \frac{1}{B}\frac{\partial v}{\partial \theta} + \frac{u}{AB}\frac{\partial B}{\partial s} + \frac{w}{R_\theta} \tag{A.16}$$

$$\varepsilon_{s\theta} = \frac{A}{B}\frac{\partial(u/A)}{\partial \theta} + \frac{B}{A}\frac{\partial(v/B)}{\partial s} \tag{A.17}$$

$$\vartheta_s = \frac{u}{R_s} - \frac{1}{A}\frac{\partial w}{\partial s} \tag{A.18}$$

$$\vartheta_\theta = \frac{v}{R_\theta} - \frac{1}{B}\frac{\partial w}{\partial \theta} \tag{A.19}$$

The mid-surface changes in curvature k_s, k_θ and twist τ are given by

$$k_s = \frac{1}{A}\frac{\partial \vartheta_s}{\partial s} + \frac{\vartheta_\theta}{AB}\frac{\partial A}{\partial \theta} \tag{A.20}$$

$$k_\theta = \frac{1}{B}\frac{\partial \vartheta_\theta}{\partial \theta} + \frac{\vartheta_s}{AB}\frac{\partial B}{\partial s} \tag{A.21}$$

$$\tau = \frac{A}{B}\frac{\partial(\vartheta_s/A)}{\partial \theta} + \frac{B}{A}\frac{\partial(\vartheta_\theta/B)}{\partial s} + \frac{1}{R_s}\left(\frac{1}{B}\frac{\partial u}{\partial \theta} - \frac{v}{AB}\frac{\partial B}{\partial s}\right) + \frac{1}{R_\theta}\left(\frac{1}{A}\frac{\partial v}{\partial s} - \frac{u}{AB}\frac{\partial A}{\partial \theta}\right) \tag{A.22}$$

According to the Donnell–Mushtari theory, the terms including Q_s and Q_θ in Eqs. (A.1) and (A.2) are neglected and Eqs. (A.6)–(A.13), respectively, simplify to $N_s = [Eh/(1-\upsilon^2)](\varepsilon_s + \upsilon\varepsilon_\theta)$, $N_\theta = [Eh/(1-\upsilon^2)](\varepsilon_\theta + \upsilon\varepsilon_s)$, $N_{s\theta} = N_{\theta s} = [Eh/2(1+\upsilon)]\varepsilon_{s\theta}$, $M_s = [Eh^3/12(1-\upsilon^2)](k_s + \upsilon k_\theta)$, $M_\theta = [Eh^3/12(1-\upsilon^2)](k_\theta + \upsilon k_s)$, $M_{s\theta} = M_{\theta s} = [Eh^3/24(1+\upsilon)]\tau$. Furthermore, the mid-surface changes in curvature k_s, k_θ and twist τ simplify to the following expressions:

$$k_s = -\frac{1}{A}\frac{\partial}{\partial s}\left(\frac{1}{A}\frac{\partial w}{\partial s}\right) - \frac{1}{AB^2}\frac{\partial A}{\partial \theta}\frac{\partial w}{\partial \theta} \tag{A.23}$$

$$k_\theta = -\frac{1}{B}\frac{\partial}{\partial \theta}\left(\frac{1}{B}\frac{\partial w}{\partial \theta}\right) - \frac{1}{BA^2}\frac{\partial B}{\partial s}\frac{\partial w}{\partial s} \tag{A.24}$$

$$\tau = -\frac{B}{A}\frac{\partial}{\partial s}\left(\frac{1}{B^2}\frac{\partial w}{\partial \theta}\right) - \frac{A}{B}\frac{\partial}{\partial \theta}\left(\frac{1}{A^2}\frac{\partial w}{\partial s}\right) \tag{A.25}$$

For a cylindrical shell, the equations of motion for u, v and w can be derived from Eqs. (A.1)–(A.3) using the following parameters; $A = a$, $B = a$, $R_s = \infty$, $R_\theta = a$ and $s = x/a$, where a is the mean radius of the shell and u, v, w and x are defined as in Fig. 1. For a conical shell, the equations of motion for u_c, v_c and w_c can be derived using $A = 1$, $B = s\sin\alpha$, $R_s = \infty$, $R_\theta = s\tan\alpha$, as well as using the change of coordinate given by $s = R/\sin\alpha$ and $R = R_0 + x_c\sin\alpha$. R, R_0, u_c, v_c, w_c and x_c are defined in Fig. 2.

Appendix B. Differential operators for the conical shell

For the conical shell, omitting the subindex c, the differential operators are given by

$$L_{11} = -\frac{\sin^2\alpha}{R^2} + \frac{\sin\alpha}{R}\frac{\partial}{\partial x} + \frac{\partial^2}{\partial x^2} + \frac{1-\upsilon}{2R^2}\frac{\partial^2}{\partial \theta^2} \tag{B.1}$$

$$\tilde{L}_{11} = \frac{1-\upsilon}{2R^2}\frac{h^2}{12}\frac{\cos^2\alpha}{R^2}\frac{\partial^2}{\partial \theta^2} - \frac{h^2}{12}\frac{\cos^2\alpha\sin^2\alpha}{R^4} \tag{B.2}$$

$$L_{12} = \frac{1+\upsilon}{2R}\frac{\partial^2}{\partial x\,\partial \theta} - \frac{3-\upsilon}{2}\frac{\sin\alpha}{R^2}\frac{\partial}{\partial \theta} \tag{B.3}$$

$$L_{13} = -\frac{\sin\alpha\cos\alpha}{R} + \frac{\upsilon\cos\alpha}{R}\frac{\partial}{\partial x} \tag{B.4}$$

$$\tilde{L}_{13} = -\frac{h^2}{12}\frac{\sin^2\alpha\cos^3\alpha}{R^4} - \frac{h^2}{12}\frac{\sin^2\alpha\cos\alpha}{12R^3} - \frac{h^2}{12}\frac{1}{R}\frac{\partial^3}{\partial x^3} + \frac{\partial}{\partial x}\frac{1-\upsilon}{2R}\frac{h^2}{12}\frac{\partial^3}{\partial x\,\partial\theta^2} - \frac{(3-\upsilon)}{2}\frac{h^2}{12}\frac{\sin\alpha\cos\alpha}{R^4}\frac{\partial^2}{\partial\theta^2} \tag{B.5}$$

$$L_{21} = \frac{3-\upsilon}{2}\frac{\sin\alpha}{R^2}\frac{\partial}{\partial\theta} + \frac{1+\upsilon}{2R}\frac{\partial^2}{\partial x\,\partial\theta} \tag{B.6}$$

$$L_{22} = -\frac{1-\upsilon}{2}\frac{\sin^2\alpha}{R^2} + \frac{1-\upsilon}{2}\frac{\sin\alpha}{R}\frac{\partial}{\partial x} + \frac{1}{R^2}\frac{\partial^2 v}{\partial\theta^2} + \frac{1-\upsilon}{2}\frac{\partial^2}{\partial x^2} \tag{B.7}$$

$$\tilde{L}_{22} = \frac{h^2}{12}\frac{\sin^2\alpha\cos^2\alpha}{R^4}\frac{3}{2}(1-\upsilon) - \frac{h^2}{12}\frac{\sin\alpha\cos^2\alpha}{R^3}\frac{\partial}{\partial x} + \frac{h^2}{12}\frac{\cos^2\alpha}{R^2}\frac{3}{2}(1-\upsilon)\frac{\partial^2}{\partial x^2} \tag{B.8}$$

$$L_{23} = \frac{\cos\alpha}{R^2}\frac{\partial}{\partial\theta} \tag{B.9}$$

$$\tilde{L}_{23} = -\frac{h^2}{12}\frac{\sin\alpha\cos\alpha}{R^4}\frac{\partial}{\partial\theta} + \frac{h^2}{12}\frac{\cos\alpha}{R^3}\frac{3}{2}(1-\upsilon)\frac{\partial^2}{\partial x\,\partial\theta} - \frac{h^2}{12}\frac{\cos\alpha}{R^2}\frac{3-\upsilon}{2}\frac{\partial^3}{\partial x^2\,\partial\theta} \tag{B.10}$$

$$L_{31} = -\frac{\sin\alpha\cos\alpha}{R^2} - \frac{\upsilon\cos\alpha}{R}\frac{\partial}{\partial x} \tag{B.11}$$

$$\tilde{L}_{31} = -\frac{h^2}{12}\frac{2\sin^3\alpha\cos\alpha}{R^4} + \frac{h^2}{12}\frac{\sin^2\alpha\cos\alpha}{R^3}\frac{\partial}{\partial x} - \frac{h^2}{12}\frac{\sin\alpha\cos^3\alpha}{R^4} + \frac{h^2}{12}\frac{\cos\alpha}{R}\frac{\partial^3}{\partial x^3} - \frac{h^2}{12}\frac{\sin\alpha\cos\alpha}{R^4}\frac{1+\upsilon}{2}\frac{\partial^2}{\partial\theta^2} - \frac{h^2}{12}\frac{\cos\alpha}{R^3}\frac{1-\upsilon}{2}\frac{\partial^3}{\partial x\,\partial\theta^2} \tag{B.12}$$

$$L_{32} = -\frac{\cos\alpha}{R^2}\frac{\partial v}{\partial\theta} \tag{B.13}$$

$$\tilde{L}_{32} = -\frac{h^2}{12}\frac{\sin\alpha\cos\alpha}{R^3}\frac{3+\upsilon}{2}\frac{\partial^2}{\partial x\,\partial\theta} + \frac{h^2}{12}\frac{\sin^2\alpha\cos\alpha}{R^4}\frac{3+\upsilon}{2}\frac{\partial}{\partial\theta} + \frac{h^2}{12}\frac{\cos\alpha}{R^2}\frac{3-\upsilon}{2}\frac{\partial^3}{\partial x^2\,\partial\theta} \tag{B.14}$$

$$L_{33} = -\frac{\cos^2\alpha}{R^2} - \frac{h^2}{12}\nabla^4 \tag{B.15}$$

$$\tilde{L}_{33} = -\frac{h^2}{12}\frac{\cos^2\alpha}{R^4}\left(2 + \cos^2\alpha + 2\frac{\partial^2}{\partial\theta^2}\right) \tag{B.16}$$

$$\nabla^4 = \nabla^2\nabla^2,\ \nabla^2 = \frac{\partial^2}{\partial x^2} + \frac{\sin\alpha}{R}\frac{\partial}{\partial x} + \frac{1}{R^2}\frac{\partial^2}{\partial\theta^2} \tag{B.17}$$

Appendix C. Elements of matrix A

The elements of matrix **A** for the cylindrical shell are given by

$$A_{11} = \Omega^2 - (k_n a)^2 - \frac{(1-\upsilon)}{2}n^2(1+\beta^2) \tag{C.1}$$

$$A_{12} = \mathrm{j}nk_n a(1+\upsilon)/2 \tag{C.2}$$

$$A_{13} = \mathrm{j}\upsilon k_n a + \mathrm{j}\beta^2[(k_n a)^3 - n^2(k_n a)(1-\upsilon)/2] \tag{C.3}$$

$$A_{21} = -A_{12} \tag{C.4}$$

$$A_{22} = \Omega^2 - (k_n a)^2(1-\upsilon)/2(1+3\beta^2) - n^2 \tag{C.5}$$

$$A_{23} = -n - \beta^2 n(k_n a)^2(3-\upsilon)/2 \tag{C.6}$$

$$A_{31} = A_{13} \tag{C.7}$$

$$A_{32} = -A_{23} \tag{C.8}$$

$$A_{33} = 1 - \Omega^2 + \beta^2\{[(k_n a)^2 + n^2]^2 + (1-2n^2)\} \tag{C.9}$$

$\Omega = \omega a/c_L$ is the dimensionless frequency parameter. Using Donnell–Mushtari theory, Eqs. (C.1), (C.3), (C.5), (C.6) and (C.9), respectively, reduce to $A_{11} = \Omega^2 - (k_n a)^2(1-\upsilon)n^2/2$, $A_{13} = \mathrm{j}\upsilon k_n a$, $A_{22} = \Omega^2 - (k_n a)^2(1-\upsilon)/2 - n^2$, $A_{23} = -n$ and $A_{33} = 1 - \Omega^2 + \beta^2[(k_n a)^2 + n^2]^2$.

Appendix D. Recurrence terms for the Donnell–Mushtari equations

The recurrence terms for the Donnell–Mushtari equations are given by

$$A_{a,1} = -\rho h\omega^2 \sin^2\alpha/D_a \tag{D.1}$$

$$A_{a,2} = -2\rho h\omega^2 R_0 \sin\alpha/D_a \tag{D.2}$$

$$A_{a,3} = -[G(m^2-1)\sin^2\alpha + \rho h\omega^2 R_0^2 - Ehn^2/2(1+\upsilon)]/D_a \tag{D.3}$$

$$A_{a,4} = -GR_0 \sin\alpha(m+1)(2m+1)/D_a \tag{D.4}$$

$$B_{a,1} = -Gn \sin\alpha(\upsilon m + m - 3 + \upsilon)/2D_a \tag{D.5}$$

$$B_{a,2} = -GR_0 n(m+1)(\upsilon+1)/2D_a \tag{D.6}$$

$$C_{a,1} = -G \sin\alpha\cos\alpha(\upsilon m - 1) \tag{D.7}$$

$$C_{a,2} = -GR_0 \sin\alpha\cos\alpha(m+1) \tag{D.8}$$

$$A_{b,1} = Gn \sin\alpha(3 + \upsilon m + m - \upsilon)/2D_b \tag{D.9}$$

$$A_{b,2} = GR_0 n(m+1)(\upsilon+1)/2D_b \tag{D.10}$$

$$B_{b,1} = -\rho h\omega^2 \sin^2\alpha/D_b \tag{D.11}$$

$$B_{b,2} = -2\rho h\omega^2 R_0 \sin\alpha/D_b \tag{D.12}$$

$$B_{b,3} = [-G(-\upsilon m^2 + m^2 - 1 + \upsilon)\sin^2\alpha - Gn^2 + \rho h\omega^2 R_0^2]/2D_b \tag{D.13}$$

$$B_{b,4} = -GR_0 \sin\alpha(m+1)(2m+1)/2D_b \tag{D.14}$$

$$C_{b,1} = Ehn\cos\alpha/(1+\upsilon)D_b \tag{D.15}$$

$$A_{c,1} = G\cos\alpha\sin^3\alpha(1 + \upsilon m - 2\upsilon)/D_c \tag{D.16}$$

$$A_{c,2} = GR_0 \cos\alpha\sin^2\alpha(2 + 3\upsilon m - 3\upsilon)/D_c \tag{D.17}$$

$$A_{c,3} = GR_0^2 \cos\alpha\sin\alpha(1 + 3\upsilon m)/D_c \tag{D.18}$$

$$A_{c,4} = \upsilon GR_0^3 \cos\alpha(m+1)/D_c \tag{D.19}$$

$$B_{c,1} = Gn\cos\alpha\sin^2\alpha/D_c \tag{D.20}$$

$$B_{c,2} = 2GR_0 n\cos\alpha\sin\alpha/D_c \tag{D.21}$$

$$B_{c,3} = GR_0^2 n\cos\alpha/D_c \tag{D.22}$$

$$C_{c,1} = -\rho h\omega^2 \sin^4\alpha/D_c \tag{D.23}$$

$$C_{c,2} = -4\rho h\omega^2 R_0 \sin^3\alpha/D_c \tag{D.24}$$

$$C_{c,3} = -\sin^2\alpha(-G\cos^2\alpha + 6\rho h\omega^2 R_0^2)/D_c \tag{D.25}$$

$$C_{c,4} = -2R_0 \sin\alpha(-G\cos^2\alpha + 2\rho h\omega^2 R_0^2)/D_c \tag{D.26}$$

$$C_{c,5} = [-D(-4m^2 + 4m^3 - m^4)\sin^4\alpha - GR_0^2\cos^2\alpha + D(2n^2m^2 + 4n^2 - 4n^2m)\sin^2\alpha - Dn^4 + \rho h\omega^2 R_0^4]/D_c \tag{D.27}$$

$$C_{c,6} = -DR_0 \sin\alpha(-2\sin^2\alpha m^2 + 2\sin^2\alpha m + \sin^2\alpha + 2n^2)(m+1)(-1+2m)/D_c \tag{D.28}$$

$$C_{c,7} = -DR_0^2(-6\sin^2\alpha m^2 + \sin^2\alpha + 2n^2)(m+2)(m+1)/D_c \tag{D.29}$$

$$C_{c,8} = 2DR_0^3 \sin\alpha(2m+1)(m+3)(m+2)(m+1)/D_c \tag{D.30}$$

where

$$D_a = GR_0^2(m+2)(m+1) \tag{D.31}$$

$$D_b = -GR_0^2(m+2)(m+1)(\upsilon-1)/2 \tag{D.32}$$

$$D_c = -DR_0^4(m+4)(m+3)(m+2)(m+1) \tag{D.33}$$

$$G = Eh/(1-\upsilon^2), D = Eh^3/12(1-\upsilon^2) \tag{D.34}$$

Appendix E. Recurrence terms for the Flügge equations

The recurrence terms for the Flügge equations are given by

$$\widetilde{A}_{a,1} = \rho h\omega^2 s^4/\widetilde{D}_a \tag{E.1}$$

$$\widetilde{A}_{a,2} = 4\rho h\omega^2 R_0 s^3/\widetilde{D}_a \tag{E.2}$$

$$\widetilde{A}_{a,3} = \{G[(m-2)^2-1]s^4 + (Gn^2\upsilon/2 + 6\rho h\omega^2 R_0^2 - Gn^2/2)s^2\}/\widetilde{D}_a \tag{E.3}$$

$$\widetilde{A}_{a,4} = sR_0(-9Gs^2m + 3Gs^2 + Gn^2\upsilon + 4Gs^2m^2 - Gn^2 + 4\rho h\omega^2 R_0^2)/\widetilde{D}_a \tag{E.4}$$

$$\widetilde{A}_{a,5} = [G(6R_0^2m^2 - 3mR_0^2 - R_0^2 - c^2h^2/2)s^2 + Dn^2\upsilon c^2/2 + \rho h\omega^2 R_0^4 + Gn^2\upsilon R_0^2/2 - Dn^2c^2/2 - Gn^2R_0^2/2]/\widetilde{D}_a \tag{E.5}$$

$$\widetilde{A}_{a,6} = GR_0^3 s(m+1)(1+4m)/\widetilde{D}_a \tag{E.6}$$

$$\widetilde{B}_{a,1} = Gs^3n(\upsilon m - \upsilon + m - 5)/2\widetilde{D}_a \tag{E.7}$$

$$\widetilde{B}_{a,2} = GR_0s^2n(3\upsilon m - \upsilon + 3m - 9)/2\widetilde{D}_a \tag{E.8}$$

$$\widetilde{B}_{a,3} = GR_0^2sn(3\upsilon m + 3m - 3 + \upsilon)/2\widetilde{D}_a \tag{E.9}$$

$$\widetilde{B}_{a,4} = GR_0^3n(m+1)(\upsilon+1)/2\widetilde{D}_a \tag{E.10}$$

$$\widetilde{C}_{a,1} = Gcs^3(-1 + \upsilon m - 2\upsilon)/\widetilde{D}_a \tag{E.11}$$

$$\widetilde{C}_{a,2} = GR_0cs^2(-2 + 3\upsilon m - 3\upsilon)/\widetilde{D}_a \tag{E.12}$$

$$\widetilde{C}_{a,3} = Gcs(2h^2n^2 + 72\upsilon mR_0^2 + h^2n^2 - 2c^2h^2 + h^2n^2\upsilon m - h^2n^2m - 24R_0^2 - h^2n^2\upsilon - 2h^2s^2m)/24\widetilde{D}_a \tag{E.13}$$

$$\widetilde{C}_{a,4} = GR_0c(m+1)(24R_0^2\upsilon - 2h^2s^2 + h^2n^2\upsilon - h^2n^2)/24\widetilde{D}_a \tag{E.14}$$

$$\widetilde{A}_{b,1} = -Gs^3n(\upsilon m - 3\upsilon + m + 1)/2\widetilde{D}_b \tag{E.15}$$

$$\widetilde{A}_{b,2} = -GR_0s^2n(3\upsilon m - 5\upsilon + 3m + 3)/2\widetilde{D}_b \tag{E.16}$$

$$\widetilde{A}_{b,3} = -sn(-36c^2D + 36G\upsilon mR_0^2 - G\upsilon h^2c^2 + 3Gh^2c^2 + 36GmR_0^2 + 36GR_0^2 - 12G\upsilon R_0^2 + 12c^2D\upsilon)/24\widetilde{D}_b \tag{E.17}$$

$$\widetilde{A}_{b,4} = -GR_0^3(m+1)(\upsilon+1)/2\widetilde{D}_b \tag{E.18}$$

$$\widetilde{B}_{b,1} = \rho h\omega^2 s^4/\widetilde{D}_b \tag{E.19}$$

$$\widetilde{B}_{b,2} = 4\rho h\omega^2 R_0 s^3/\widetilde{D}_b \tag{E.20}$$

$$\widetilde{B}_{b,3} = G(-1+\upsilon-\upsilon(m-2)^2 + (m-2)^2)s^4/2 + (6\rho h\omega^2 R_0^2 - Gn^2)s^2/\widetilde{D}_b \tag{E.21}$$

$$\widetilde{B}_{b,4} = -R_0s(-8\rho h\omega^2 R_0^2 - 3s^2G + 4Gn^2 + 4G\upsilon s^2m^2 - 9G\upsilon s^2m + 3G\upsilon s^2 - 4s^2Gm^2 + 9s^2Gm)/2\widetilde{D}_b \tag{E.22}$$

$$\widetilde{B}_{b,5} = [(-3G\upsilon R_0^2 m^2 - c^2 D\upsilon/2 + Dc^2 + c^2 D/2 - GR_0^2/2 + G\upsilon R_0^2/2 - D\upsilon c^2 - Gh^2 mc^2/8 + \upsilon mR_0^2 3G/2 - 3/2GmR_0^2 + 1/8Gh^2\upsilon mc^2 + 3GR_0^2 mq + 1/24c^2 Gh^2 m^2 - 1/24Gh^2\upsilon c^2 m^2 - 3/2c^2 Dm + c^2 Dm^2 + 3/2c^2 D\upsilon m - c^2 D\upsilon m^2)s^2 - Gn^2 R_0^2 + \rho h\omega^2 R_0^4]/\widetilde{D}_b \tag{E.23}$$

$$\widetilde{B}_{b,6} = -R_0 s(m+1)(24GR_0^2 m + 24c^2 Dm + c^2 Gh^2 m + 6GR_0^2 - c^2 Gh^2 - 6c^2 D)(\upsilon - 1)/12\widetilde{D}_b \tag{E.24}$$

$$\widetilde{C}_{b,1} = -Gcs^2 n/\widetilde{D}_b \tag{E.25}$$

$$\widetilde{C}_{b,2} = -2GR_0 csn/\widetilde{D}_b \tag{E.26}$$

$$\widetilde{C}_{b,3} = cn(-24GR_0^2 + 24Dm^2 s^2 + 4Gh^2\upsilon ms^2 + 2n^2 Gh^2 + 3Gh^2 s^2 - 24n^2 D - Gh^2\upsilon m^2 s^2 - 6Gh^2 ms^2 + 24c^2 D - 2c^2 Gh^2 - 3Gh^2\upsilon s^2 + Gh^2 m^2 s^2)/24\widetilde{D}_b \tag{E.27}$$

$$\widetilde{C}_{b,4} = -R_0 csn(m+1)(-48Dm - 2Gh^2 m + 2Gh^2\upsilon m - 24D - 3Gh^2\upsilon + 5Gh^2)/24\widetilde{D}_b \tag{E.28}$$

$$\widetilde{C}_{b,5} = -DR_0^2 cn(m+2)(m+1)(1+\upsilon)/2\widetilde{D}_b \tag{E.29}$$

$$\widetilde{A}_{c,1} = -Gcs^3(1 + \upsilon m - 2\upsilon)/\widetilde{D}_c \tag{E.30}$$

$$\widetilde{A}_{c,2} = -GR_0 cs^2(2 + 3\upsilon m - 3\upsilon)/\widetilde{D}_c \tag{E.31}$$

$$\widetilde{A}_{c,3} = [-1/12cD(24 - 36m - 12m^3 + 36m^2)s^3 - 1/12c(12GR_0^2 - 6Dn^2\upsilon + c^2 Gh^2 + 6Dn^2\upsilon m + 36G\upsilon R_0^2 m - Dn^2 - 6Dn^2 m)s]/\widetilde{D}_c \tag{E.32}$$

$$\widetilde{A}_{c,4} = -1/2R_0 c(m+1)(-Dn^2 + 6Dms^2 - 2Ds^2 - 6Dm^2 s^2 + Dn^2\upsilon + 2G\upsilon R_0^2)/\widetilde{D}_c \tag{E.33}$$

$$\widetilde{A}_{c,5} = 3DR_0^2 cs(m+2)(m+1)m/\widetilde{D}_c \tag{E.34}$$

$$\widetilde{A}_{c,6} = DR_0^3 c(m+3)(m+2)(m+1)/\widetilde{D}_c \tag{E.35}$$

$$\widetilde{B}_{c,1} = -Gcs^2 n/\widetilde{D}_c \tag{E.36}$$

$$\widetilde{B}_{c,2} = -2GR_0 csn/\widetilde{D}_c \tag{E.37}$$

$$\widetilde{B}_{c,3} = -cn(D\upsilon m^2 s^2 + 6Dms^2 + 2GR_0^2 - 3Dm^2 s^2 - 3Ds^2 - Ds^2\upsilon)/2\widetilde{D}_c \tag{E.38}$$

$$\widetilde{B}_{c,4} = -Dcn(m+1)sR_0(3 + 2\upsilon m + \upsilon - 6m)/2\widetilde{D}_c \tag{E.39}$$

$$\widetilde{B}_{c,5} = -DR_0^2 cn(m-1)m(-3+\upsilon)/2\widetilde{D}_c \tag{E.40}$$

$$\widetilde{C}_{c,1} = \rho h\omega^2 s^4/\widetilde{D}_c \tag{E.41}$$

$$\widetilde{C}_{c,2} = 4\rho h\omega^2 R_0 s^3/\widetilde{D}_c \tag{E.42}$$

$$\widetilde{C}_{c,3} = -s^2(c^2 G - 6\rho h\omega^2 R_0^2)/\widetilde{D}_c \tag{E.43}$$

$$\widetilde{C}_{c,4} = -2R_0 s(c^2 G - 2\rho h\omega^2 R_0^2)/\widetilde{D}_c \tag{E.44}$$

$$\widetilde{C}_{c,5} = [D(4m^3 - m^4 - 4m^2)s^4 + D(mc^2 - c^2 m - 2c^2 - 4n^2 m + 2n^2 m^2 + 4n^2)s^2 + \rho h\omega^2 R_0^4 - c^2 GR_0^2 + Dc^2 n^2 + Dn^2 c^2 - c^4 D - Dn^4]/\widetilde{D}_c \tag{E.45}$$

$$\widetilde{C}_{c,6} = DR_0 s(m+1)(-12s^2 - 48s^2 m^3 + 72s^2 m^2 - 24n^2 - 12c^2 + 48n^2 m + 12c^2)/12\widetilde{D}_c \tag{E.46}$$

$$\widetilde{C}_{c,7} = DR_0^2(-6s^2 m^2 + s^2 + 2n^2)(m+2)(m+1)/\widetilde{D}_c \tag{E.47}$$

$$\widetilde{C}_{c,8} = -2DR_0^3 s(2m+1)(m+3)(m+2)(m+1)/\widetilde{D}_c \tag{E.48}$$

where

$$\widetilde{D}_a = -GR_0^4(m+2)(m+1) \tag{E.49}$$

$$\widetilde{D}_b = R_0^2(12GR_0^2 + 24Dc^2 + Gh^2c^2)(m+2)(m+1)(\upsilon-1)/24 \tag{E.50}$$

$$\widetilde{D}_c = DR_0^4(m+4)(m+3)(m+2)(m+1) \tag{E.51}$$

$$c = \cos\alpha, \quad s = \sin\alpha \tag{E.52}$$

References

[1] A.W. Leissa, in: *Vibration of Shells*, American Institute of Physics, New York, 1993.
[2] H. Saunders, E.J. Paslay, P.R. Wisniewski, Vibrations of conical shells, *J. Acoust. Soc. Am.* 32 (1960) 765–772.
[3] H. Garnet, J. Kempner, Axisymmetric free vibration of conical shells, *J. Appl. Mech.* 31 (1964) 458–466.
[4] R.A. Newton, Free vibrations of rocket nozzles, *Am. Inst. Aeronaut. Astronaut. J.* 4 (1966) 1303–1305.
[5] C.C. Siu, C.W. Bert, Free vibrational analysis of sandwich conical shells with free edges, *J. Acoust. Soc. Am.* 47 (1970) 943–945.
[6] T. Irie, G. Yamada, Y. Kaneko, Free vibration of a conical shell with variable thickness, *J. Sound Vib.* 82 (1982) 83–94.
[7] L. Tong, Free vibration of orthotropic conical shells, *Int. J. Eng. Sci.* 31 (1993) 719–733.
[8] Y.P. Guo, Normal mode propagation on conical shells, *J. Acoust. Soc. Am.* 96 (1994) 256–264.
[9] M. Lashkari, V.I. Weingarten, Vibrations of segmented shells, *Exp. Mech.* 13 (1973) 120–125.
[10] A. Kalnins, Free vibration of rotationally symmetric shells, *J. Acoust. Soc. Am.* 36 (1964) 1355–1365.
[11] J.L. Rose, R.W. Mortimer, A. Blum, Elastic-wave propagation in a joined cylindrical–conical–cylindrical shell, *Exp. Mech.* 13 (1973) 150–156.
[12] W.C.L. Hu, J.P. Raney, Experimental and analytical study of vibrations of joined shells, *AIAA J.* 5 (1967) 976–980.
[13] T. Irie, G. Yamada, Y. Muramoto, Free vibration of joined conical–cylindrical shells, *J. Sound Vib.* 95 (1984) 31–39.
[14] E. Efraim, M. Eisenberger, Exact vibration frequencies of segmented axisymmetric shells, *Thin-Walled Struct.* 44 (2006) 281–289.
[15] B.P. Patel, M. Ganapathi, S. Kamat, Free vibration characteristics of laminated composite joined conical–cylindrical shells, *J. Sound Vib.* 237 (2000) 920–930.
[16] MSC/NASTRAN Basic Dynamic Analysis User's Guide, 1997.
[17] A.S. Kadi, A Study and Comparison of the Equations of Thin Shell Theories, Ph.D. Thesis, Ohio State University, Columbus, 1970.
[18] K. Kraus, in: *Thin Elastic Shells*, Wiley, New York, 1967.